Open Access Full Text Article

ORIGINAL RESEARCH

Colonic inflammation affects myenteric alpha-synuclein in nonhuman primates

Henry Resnikoff[1,]*
Jeanette M Metzger[1,2,]*
Mary Lopez[1]
Viktoriya Bondarenko[1]
Andres Mejia[1]
Heather A Simmons[1]
Marina E Emborg[1–3]

[1]Preclinical Parkinson's Research Program, Wisconsin National Primate Research Center, University of Wisconsin – Madison, Madison, WI, USA; [2]Cellular and Molecular Pathology Graduate Program, University of Wisconsin – Madison, Madison, WI, USA; [3]Department of Medical Physics, University of Wisconsin – Madison, Madison, WI, USA

*These authors contributed equally to this work

Background: Parkinson's disease (PD) patients frequently present gastrointestinal (GI) dysfunction that, in many cases, predates the onset of motor symptoms. In PD, the pre-synaptic protein alpha-synuclein (α-syn) undergoes pathological changes, including phosphorylation and aggregation leading to the formation of Lewy bodies, which can be found in neurons of the enteric nervous system (ENS). Inflammation has been proposed as a possible trigger of α-syn pathology. Interestingly, patients with inflammatory bowel disease and irritable bowel syndrome, conditions associated with GI inflammation, are at higher risk of developing PD. Captive common marmosets *(Callithrix jacchus)* develop colitis, providing a natural platform to assess the relationship between α-syn pathology and GI inflammation.

Materials and Methods: Sections of proximal colon from marmosets with colitis (n=5; 5.3 ±2.3 years old; 4 male) and normal controls (n=5; 4.1±1.6 years old; 1 male) were immunostained against protein gene product 9.5 (PGP9.5), human leukocyte antigen DR (HLA-DR), cluster of differentiation 3 (CD3), cluster of differentiation 20 (CD20), glial fibrillary acidic protein (GFAP), 8-hydroxy-2'-deoxyguanosine (8-OHdG), α-syn, and serine 129 phosphorylated α-syn (p-α-syn). Immunoreactivity of each staining in the myenteric plexus was quantified using NIH ImageJ software.

Results: Marmosets with colitis had significantly increased expression of inflammatory markers (HLA-DR, $p<0.02$; CD3, $p<0.008$), oxidative stress (8-OHdG, $p<0.05$), and p-α-syn ($p<0.02$) and decreased expression of α-syn ($p<0.04$) in the colonic myenteric ganglia compared to normal, healthy controls.

Conclusion: Colonic inflammation is associated with changes in α-syn expression and phosphorylation in the myenteric plexus of common marmosets. Future evaluation of the vagus nerve and brain of animals with colitis will be key to assess the contribution of colitis-induced ENS α-syn pathology to PD-like pathology in the brain.

Keywords: Lewy bodies, common marmosets, colitis, Parkinson's disease, phosphorylated alpha-synuclein, HLA-DR

Plain language summary

In this study, we learned that inflammation in monkeys' gastrointestinal (GI) tract affects the neurons that innervate the colon. Specifically, the protein named alpha-synuclein becomes "phosphorylated", a change associated with Parkinson's disease (PD). This intriguing result supports future work investigating the role of GI inflammation in the onset of PD.

Introduction

Colonic inflammation is a prominent feature of numerous conditions including irritable bowel syndrome (IBS),[1] inflammatory bowel disease (IBD),[2] celiac disease,[3] and colitis associated with chemical exposure[4] or infectious pathogens.[5,6] Markers of inflammation

Correspondence: Marina E Emborg
Preclinical Parkinson's Research Program, Wisconsin National Primate Research Center, University of Wisconsin–Madison, 1220 Capitol Court, Madison, WI 53715, USA
Tel +1 608 262 9714
Fax +1 608 263 3524
Email emborg@primate.wisc.edu

113

are also found in the colon[7] and stool[8] of Parkinson's disease (PD) patients; in recent years, IBD[9–12] and IBS[13] have been linked to increased risk of developing PD. Gastrointestinal (GI) dysfunction, in particular constipation, is a common non-motor symptom of PD known to predate the onset of the typical PD motor symptoms.[14,15]

α-Synuclein (α-syn) is a presynaptic protein ubiquitously distributed in neurons of the central and peripheral nervous systems.[16,17] It is usually found in a soluble, monomeric form, but in pathological conditions, α-syn becomes phosphorylated, aggregated, and, in PD, combined with other proteins like tau to form Lewy bodies (LBs).[18] Inflammation and oxidative stress are proposed to trigger α-syn phosphorylation and aggregation,[19–21] thus facilitating the development of PD pathology. LBs are found in the central and peripheral nervous systems of PD patients, including the enteric nervous system (ENS), yet their role in PD neurodegeneration is still unclear.

The ENS of nonhuman primates such as common marmosets (*Callithrix jacchus)* has an organization similar to humans. The neuronal cell bodies of the ENS are grouped into ganglia that are embedded in the wall of the GI tract in the net-like submucosal and myenteric plexuses. ENS neurons express, and often co-express, diverse neurotransmitters including acetylcholine, dopamine, and serotonin. Common marmosets in captivity occasionally develop colitis[22] which is histologically defined by inflammation within the colon wall, predominantly in the lamina propria, and may be accompanied by weight loss and malabsorption with or without diarrhea. The Wisconsin National Primate Research Center (WNPRC) has banked formalin-fixed, paraffin-embedded (FFPE) colon samples from common marmosets with and without colitis. In this report, we utilized this resource to carry out a retrospective study to test the hypothesis that α-syn expression in the myenteric plexus is modified by colonic inflammation.

Material and methods
Ethics statement
This experiment was performed in strict accordance with the recommendations in the National Research Council Guide for the Care and Use of Laboratory Animals (2011) in an AAALAC accredited facility, the WNPRC at the University of Wisconsin–Madison. The monkey tissues were obtained from the WNPRC tissue bank. These monkeys were originally assigned to and euthanized under the University of Wisconsin–Madison Institutional Animal Care and Use Committee (IACUC) experimental

protocols G00305, G005273, G00526, G00101, G00140, G00296, WPRC00, and G00474. Experimental procedures were approved by the IACUC of the University at the Wisconsin–Madison. All efforts were made to minimize the number of animals used and to ameliorate any distress.

Human brain tissue was obtained from the Wisconsin Alzheimer's Disease Research Center Brain Bank following documented review and approval from the Institutional Review Board. All tissue in the brain bank is collected following written informed consent by the patient, in accordance with the Declaration of Helsinki.

Tissues
FFPE samples of proximal colon from adult common marmosets with colitis (n=5; 5.3±2.3 years old; 4 male) and normal controls (n=5; 4.1±1.6 years old; 1 male) were used in this study (Table 1). Criteria for selection included FFPE colonic samples in cross-section orientation with minimal antemortem or postmortem ectasia (dilation), visible myenteric plexus, and the presence of inflammation in the colonic wall (colitis; see below for colitis scoring information) or lack thereof (normal control). Subjects with confounding pathologies, such as diseases that affect the nervous system, immune system, or intestinal function were excluded.

Anatomical evaluation and colitis score
A representative proximal colon section from each subject was stained with hematoxylin and eosin (HE) and blindly evaluated for general histologic changes and the presence of inflammation in the colonic wall by board-certified veterinary pathologists familiar with the histologic findings common to the WNPRC marmoset colony (H.A.S., A.M.). Inflammation was scored using a scale of 1–4 (1=no inflammation, 2=mild, 3=moderate, 4=severe) with increments of 0.5 depending on the degree of inflammatory cell infiltration into the lamina propria, glandular displacement, and dysmorphology.

General immunohistochemistry
FFPE proximal colon was sectioned at 5 µm and immunostained against protein gene product 9.5 (PGP9.5), human leukocyte antigen DR (HLA-DR), cluster of differentiation 3 (CD3), cluster of differentiation 20 (CD20), glial fibrillary acidic protein (GFAP), 8-hydroxy-2'-deoxyguanosine (8-OHdG), α-syn, and serine 129 phosphorylated α-syn (p-α-syn) following previously validated

Table 1 Pathological descriptions of colitis per subject

Animal no.	Age (yr)	Sex	Weight (g)	Colitis score	Pathological description	Diarrhea*
cj1	3.2	F	270	2 (mild)	Mainly lymphocytes present with some plasma cells; mild edema	Not recorded
cj2	2.7	M	340	2 (mild)	Mostly lymphocytes and plasma cells present, scattered neutrophils; expansion of the lamina propria and displacement of the glands	Infrequent (once every few months)
cj3	8	M	305	3 (moderate)	Submucosal infiltration with a mix of plasma cells, lymphocytes, and eosinophils; inflammation expands the lamina propria	Approx. 4 episodes per month for 1.0 yr until the month prior to death, then almost daily
cj4	5.7	M	355	3 (moderate)	Mostly lymphocytes and plasma cells present with few eosinophils; inflammatory cells present within the glands	Approx. 5 episodes per month for 1.5 yr prior to death
cj5	7	M	361	3.5 (Moderate to severe)	Mainly lymphocytes present and a few plasma cells; abscessation within the crypts; lymphocytic inflammation expands the submucosa	Not recorded
cj6	3.1	F	313	1 (no colitis)	No evidence of colitis	Not recorded
cj7	5.0	M	281	1 (no colitis)	No evidence of colitis	Approx. 10 episodes per month for 2 months prior to death
cj8	3.0	F	449	1 (no colitis)	No evidence of colitis	Not recorded
cj9	2.7	F	460	1 (no colitis)	No evidence of colitis	Very infrequent (1 or 2 days per year for 2 years prior to death)
cj10	3.2	F	421	1 (no colitis)	No evidence of colitis	Not recorded

Notes: *Marmosets are housed in family groups and diarrhea is recorded for the entire group if a specific individual cannot be identified as the origin.
Abbreviations: yr, year; F, female; M, male; g, gram.

methods[23] (see Table 2 for full list of primary antibody information).

Briefly, slides were deparaffinized and treated for heat antigen retrieval in a microwave for 6 mins at 100% power followed by 3 mins at 60% power and left to cool for 1 hr at room temperature. Tissue sections were blocked with either Super Block (ScyTek, Logan, UT, USA) or appropriate species serum and incubated in primary antibodies overnight at 4° C. The sections were then incubated in appropriate biotinylated secondary antibody (1:200), followed by avidin-biotin-complex peroxidase (VECTASTAIN Elite ABC HRP Kit, Vector Laboratories, Burlingame, CA, USA) or avidin-biotin-complex alkaline phosphatase kit (VECTASTAIN ABC-AP Staining Kit, Vector Laboratories, Burlingame, CA, USA), and visualized with either a commercial 3,3′-diaminobenzidine (DAB) kit (colon tissue; all antibodies other than 8-OHdG) (Vector Laboratories, Burlingame, CA, USA), VectorBLACK kit (colon tissue; 8-OHdG) (Vector Laboratories, Burlingame, CA, USA), or a NovaRED kit (brain tissue) (Vector Laboratories, Burlingame, CA, USA). In order to evaluate for the existence of α-syn aggregates, tissue was incubated with proteinase K (PK) dissolved in PBS (1:1000) for 15 mins prior to α-syn primary antibody incubation (PK α-syn). All sections were counterstained with hematoxylin, dehydrated, and coverslipped (Cytoseal mounting medium, Thermo Scientific, Waltham, MA, USA). Human brain tissue at the level of the substantia nigra from a PD patient was used as a positive control for α-syn and p-α-syn (Figure S1) immunostaining; staining was performed in parallel with marmoset colon tissue. Colon cancer tissue from a rhesus macaque was used as a positive control for the 8-OHdG antibody. Negative controls were processed in parallel by omitting the primary antibodies during the immunostaining procedures.

Immunofluorescence

Double-label immunofluorescence was performed to visualize colocalization of p-α-syn with subtypes of ENS

Table 2 Primary antibodies used for general immunohistochemistry and immunofluorescence

Antigen	Marker	Company	Species	Catalog no.	Lot no.	Dilution
PGP9.5	panneuronal, soma and processes (brightfield)	Millipore	Rabbit	AB1761	MG1898214	1:400
PGP9.5	panneuronal, soma and processes (fluorescence)	Abcam	Mouse	AB8189	NG1898217	1:1000
HLA-DR	antigen presenting cell surface	Dako	Mouse	M0746	00051226	1:200
CD3	T cells	Dako	Mouse	M7254	20043703	1:100
CD20	B cells	Thermo-Scientific	Rabbit	RB9013-PO	9013P1705F	1:100
GFAP	enteric glial cells	Dako	Rabbit	20334	00015316	1:100
8-OHdG	oxidative stress; somatic and nuclear	Abcam	Mouse	AB48508	GR218391-16	1:50
α-syn	pre-synaptic protein	Abcam	Rabbit	AB138501	GR183898-9	1:800
p-α-syn	α-syn phosphorylated at serine 129	Wako	Mouse	015–25191	LKM6409	1:400
VIP	VIP-ergic neurons	Santa-Cruz Biotechnology	Rabbit	Sc20727	H3012	1:400
TH	catecholaminergic neurons	Immunostar	Mouse	22941	1240001	1:400

Abbreviations: PGP9.5, protein gene product 9.5; HLA-DR, human leukocyte antigen DR; CD3, cluster of differentiation 3; CD20, cluster of differentiation 20; GFAP, glial fibrillary acidic protein; 8-OHdG, 8-hydroxy-2'-deoxyguanosine; α-syn, alpha-synuclein; p-α-syn, alpha-synuclein phosphorylated at serine 129; VIP, vasoactive intestinal peptide; TH, tyrosine hydroxylase.

neurons including catecholaminergic (tyrosine hydroxylase; TH) and vasoactive intestinal peptide (VIP)-ergic and to visualize colocalization of α-syn and PGP9.5 (see Table 2 for full list of primary antibody information). Slides were deparaffinized and treated for heat antigen retrieval in a microwave for 6 mins at 100% power followed by 3 mins at 60% power and left to cool for 30 mins at room temperature. Tissue was blocked with 5% donkey serum and 2% BSA solution and incubated in primary antibodies overnight at 4°C. The sections were then incubated with Alexa Fluor-conjugated secondary antibody (1:1000) against the appropriate species and cover slipped with mounting medium with DAPI (Vector Laboratories, Burlingame, CA). Negative controls were performed in parallel by omitting the primary antibodies.

Quantification of immunostaining

Immunostaining in myenteric ganglia was blindly quantified using NIH ImageJ software in images obtained with a Zeiss Axio Imager M2 equipped with a QImaging camera. Every myenteric ganglion from each immunostained colon tissue section was captured at 63x. To equalize the number of ganglia analyzed per subject, 8 pictures were randomly selected using a random number generator (Google Random Number Generator). In each photomicrograph, DAB color was separated from hematoxylin counterstain with the ImageJ Color Deconvolution filter. ImageJ was calibrated using a step tablet and gray scale values were converted to OD units using the Rodbard

function. The ganglia were outlined and the percent area of each ganglion with immunoreactivity above threshold (%AAT) was measured. The threshold is a minimum gray scale value (darkness of the immunoreactivity) of each pixel applied as a cutoff for inclusion in the %AAT calculation. The threshold was calculated by averaging the optimal individual threshold that best represents the immunoreactivity (-ir) for 2–4 photomicrographs of immunostained tissue sections.

Statistics

Data collection and analysis were performed by investigators blind to the treatment groups. Statistical analysis was performed using GraphPad Prism (version 5.0f, GraphPad Software). Results are presented as mean ±SEM. For comparisons between the two groups, equality of variances was determined using an F-test. The p-values for data sets with similar variances for each group (PGP9.5, 8-OHdG, α-syn, PK α-syn) were calculated using a two-tailed, independent samples Student's t-test. The p-values for data sets with significantly difference variances for each group (HLA-DR, CD20, CD3, GFAP, p-α-syn) were calculated using the Mann–Whitney rank sum test. A $p < 0.05$ was considered significant.

To compare all variables (colitis score and %AAT of each immunostaining) across animals, we first normalized the values by creating a relative index score for each variable per animal, before plotting the results. The

relative index score was calculated as a percentage of the highest value for each variable.

Results

HE-stained proximal colon sections of marmoset monkeys with colitis were characterized by inflammatory cell infiltration (lymphocytic, lymphoplasmacytic, or lymphoplasmacytic with some eosinophils) of the lamina propria causing mucosal expansion, glandular displacement, glandular dysplasia with variable goblet cell loss, and occasional gland abscessation (Figure 1A and B), as compared to controls (Table 1). The ganglia in the myenteric plexus contained neuronal soma with large, round, euchromatic nuclei, and prominent nucleoli (Figure 1). Expression of the panneuronal marker PGP9.5 was uniformly present throughout neuronal cell bodies and processes in the myenteric plexus and in nerve fibers running between muscle fibers and mucosa (Figure 1C). PGP9.5-immunoreactivity (-ir), quantified as percent area above threshold (%AAT) in myenteric ganglia, was similar between control (78.4 ± 4.3) and colitis (69.3 ± 6.5) animals ($p > 0.3$; Figure 1C).

Expression of HLA-DR, a marker of antigen presenting cells, was observed on the surface of cells with circular/ovoid shape in all animals, as well as on macrophage-like cells (Figure 2A). HLA-DR-ir %AAT quantification confirmed the presence of significantly increased inflammatory cell infiltration into colonic myenteric ganglia in colitis animals (4.7 ± 2.8) compared to healthy controls (0.5 ± 0.3) ($p < 0.02$; Figure 2A). Immunostaining for the immune cell markers CD3 (T cells) and CD20 (B cells) was performed to interrogate the cell types involved in colitis. CD3 and CD20 cells were present in Peyer's patches of both groups and were either occasionally or frequently localized in the lamina propria of control or colitis animals, respectively (Figure 2B and C). Within myenteric ganglia, colitis animals (0.4 ± 0.1) had increased CD3-ir compared to control animals (0.002 ± 0.0008) ($p < 0.008$; Figure 2B). In contrast, CD20-ir %AAT was unchanged between groups (control: 0.004 ± 0.002; colitis: 0.02 ± 0.007; $p > 0.4$; Figure 2C), implicating CD3+ T cells in colitis-associated alterations to colonic myenteric ganglia. GFAP immunostaining identified enteric glial cells tightly packed around neurons in myenteric ganglia (Figure 2D). GFAP-ir was greater and more variable in colitis animals (28.1 ± 8.8) compared to controls (9.3 ± 2.0), showing a trend toward increased gliosis accompanying colitis ($p > 0.09$; Figure 2D). Further, the expression of the oxidative stress marker 8-OHdG was increased in the

colitis animal group (14.5 ± 3.3) compared to controls (4.7 ± 2.4) ($p < 0.05$; Figure 2E).

α-Syn-ir was found within the myenteric ganglia and in nerve fibers running through the muscle and mucosal layers (Figure 3A), colocalizing with PGP9.5 (Figure S2). Quantification of α-syn-ir showed less %AAT in the colitis group (76.8 ± 5.6) as compared to the control (91.6 ± 2.0) ($p < 0.04$; Figure 3A). This decrease in α-syn-ir %AAT was not associated with altered cellular localization of α-syn-ir (in cell body vs neurites, etc.) in the colitis group compared to the controls (Figure S2). Immunostaining for p-α-syn was variably present in neurons in the myenteric ganglia of control and colitis animals (Figure 3B). Quantification showed significantly greater ($p < 0.02$) p-α-syn-ir %AAT in the animals with colitis (8.4 ± 5.1) compared to controls (0.08 ± 0.05). After establishing the presence of p-α-syn, colon sections were subjected to proteinase K digestion prior to α-syn immunostaining to determine whether insoluble α-syn aggregates (PK α-syn) were present. No differences were found between groups for PK α-syn-ir %AAT (control: 4.0 ± 1.8; colitis: 6.9 ± 2.9; $p > 0.4$; Figure 3C).

To assess whether p-α-syn was associated with any specific neuronal phenotype, double-label immunofluorescence was performed in colitis animals using antibodies against p-α-syn and the neuronal markers TH and VIP, which stain catecholaminergic and VIP-ergic neurons, respectively (Figure 4A and B). We found that p-α-syn-ir colocalized with both TH-ir and VIP-ir in myenteric ganglia neurons of animals with colitis.

To visualize the relationship between colitis score, inflammation and oxidative stress markers, and α-syn, a relative index plot was created (Figure 4C). In this plot, each variable (eg, colitis score, HLA-DR %AAT, p-α-syn %ATT, etc.) was normalized to the animal with the highest value for that variable. As described above, colitis animals showed higher relative index scores for p-α-syn, inflammation, and oxidative stress markers compared to controls, but similar scores for PGP9.5 and α-syn.

Discussion

The present study in common marmosets indicates that colitis-associated inflammation is concomitant to alterations in α-syn and p-α-syn expression in colonic myenteric ganglia. To the best of our knowledge, this is the first report of the effects of naturally occurring colitis on enteric α-syn in nonhuman primates.
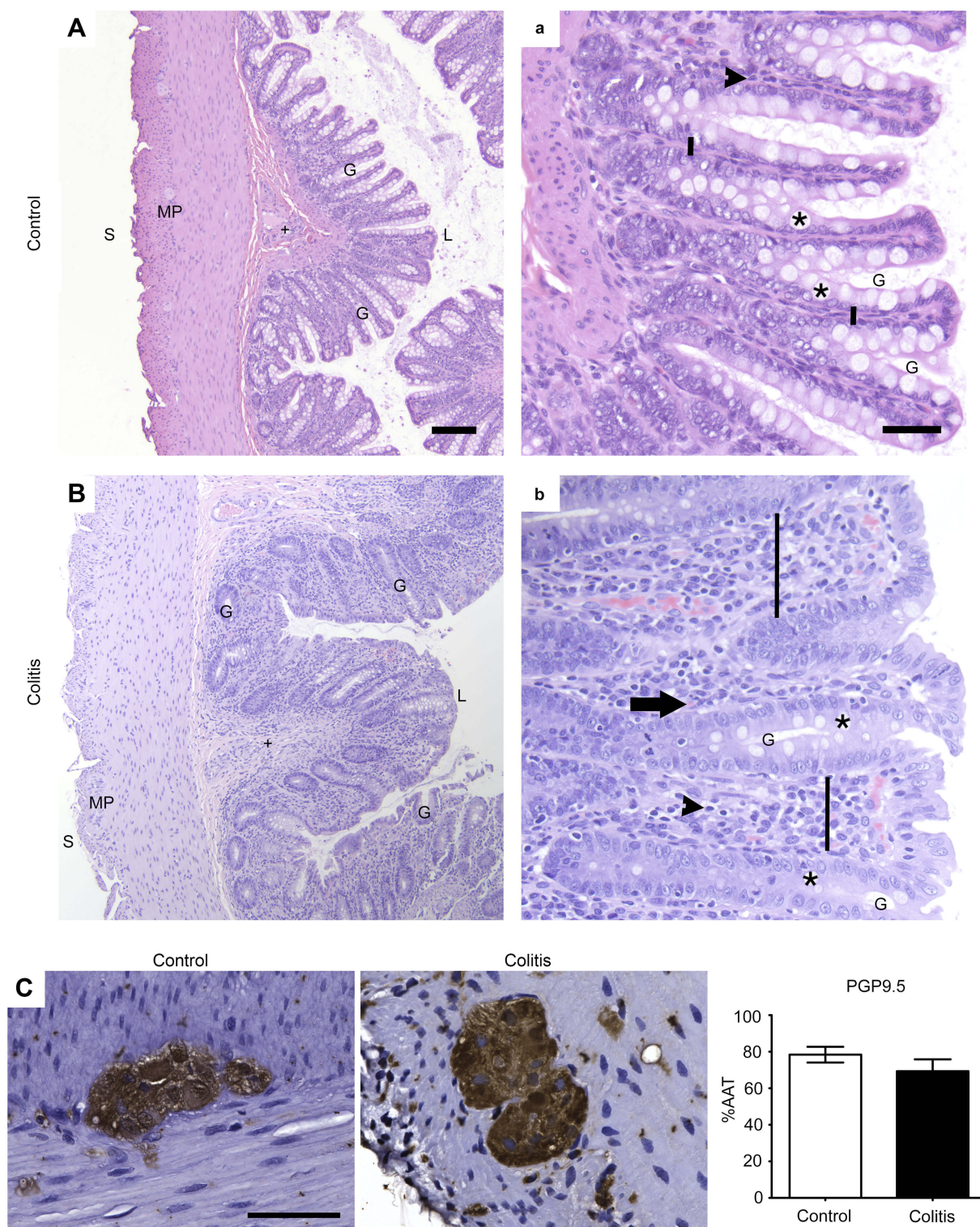
Figure 1 General colon anatomy of common marmosets with normal or colitis conditions. (**A**,a; **B**,b) Colon sections from marmosets were stained with HE and evaluated for the presence of colitis (Table 1; A,B =10×, scale bar =100 μm; a,b =40×, scale bar =50 μm). G, gland; L, luminal surface; MP, myenteric plexus; S, serosal surface; +, submucosa; *, goblet cell; black arrowhead, resident lymphocyte; black arrow, eosinophil; vertical black bar, lamina propria between adjacent glands. Note inflammatory infiltration of the lamina propria causing mucosal expansion, glandular displacement, and glandular dysplasia with decreased goblet cells in the tissue from a marmoset with colitis (**B**,b) compared to a normal control (**A**,a). (**C**) Immunohistochemical staining of neurons (PGP9.5) and quantification of percentage of total area of myenteric ganglia immunoreactive (%AAT) for PGP9.5 with comparison between groups analyzed by Student's *t*-test showing no difference between groups (*p*>0.2; scale bar=50 μm). n=5 per group.
**Abbreviations:** HE, hematoxylin and eosin; PGP9.5, protein gene product 9.5; %AAT, percent area above threshold.
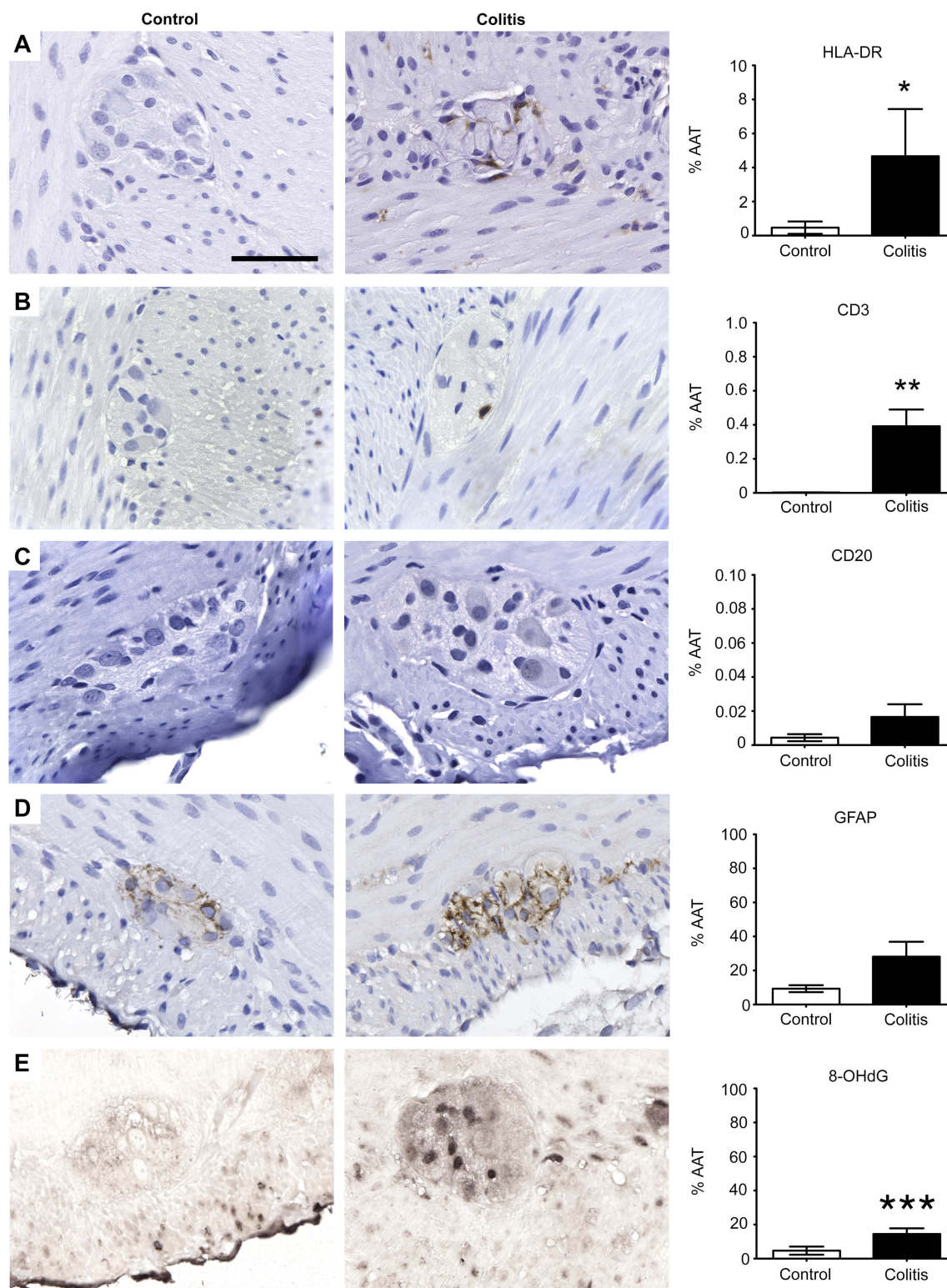
Figure 2 Inflammation and oxidative stress markers are elevated in the colonic myenteric plexus of marmosets with colitis. Immunohistochemical staining of (**A**) antigen presenting cells (HLA-DR), (**B**) T cells (CD3), (**C**) B cells (CD20), (**D**) enteric glial cells (GFAP), and (**E**) oxidative stress (8-OHdG) and quantification of percentage of total area of myenteric ganglia immunoreactive (%AAT) for each marker. Comparisons between groups were analyzed by either Student's *t*-test (8-OHdG) or Mann–Whitney (HLA-DR, CD20, CD3, and GFAP) based on F-tests for equality of variances. HLA-DR (*$p<0.02$), CD3 (**$p<0.008$), and 8-OHdG (***$p<0.05$) %AAT were significantly greater in colitis animals than controls. GFAP showed a trend toward higher %AAT in controls ($p>0.09$). CD20 %AAT was similar between groups ($p>0.4$). Scale bar =50 μm. n=5 per group.
Abbreviations: HLA-DR, human leukocyte antigen DR; CD3, cluster of differentiation 3; CD20, cluster of differentiation 20; GFAP, glial fibrillary acid protein; 8-OHdG, 8-hydroxy-2'-deoxyguanosine; %AAT, percent area above threshold.
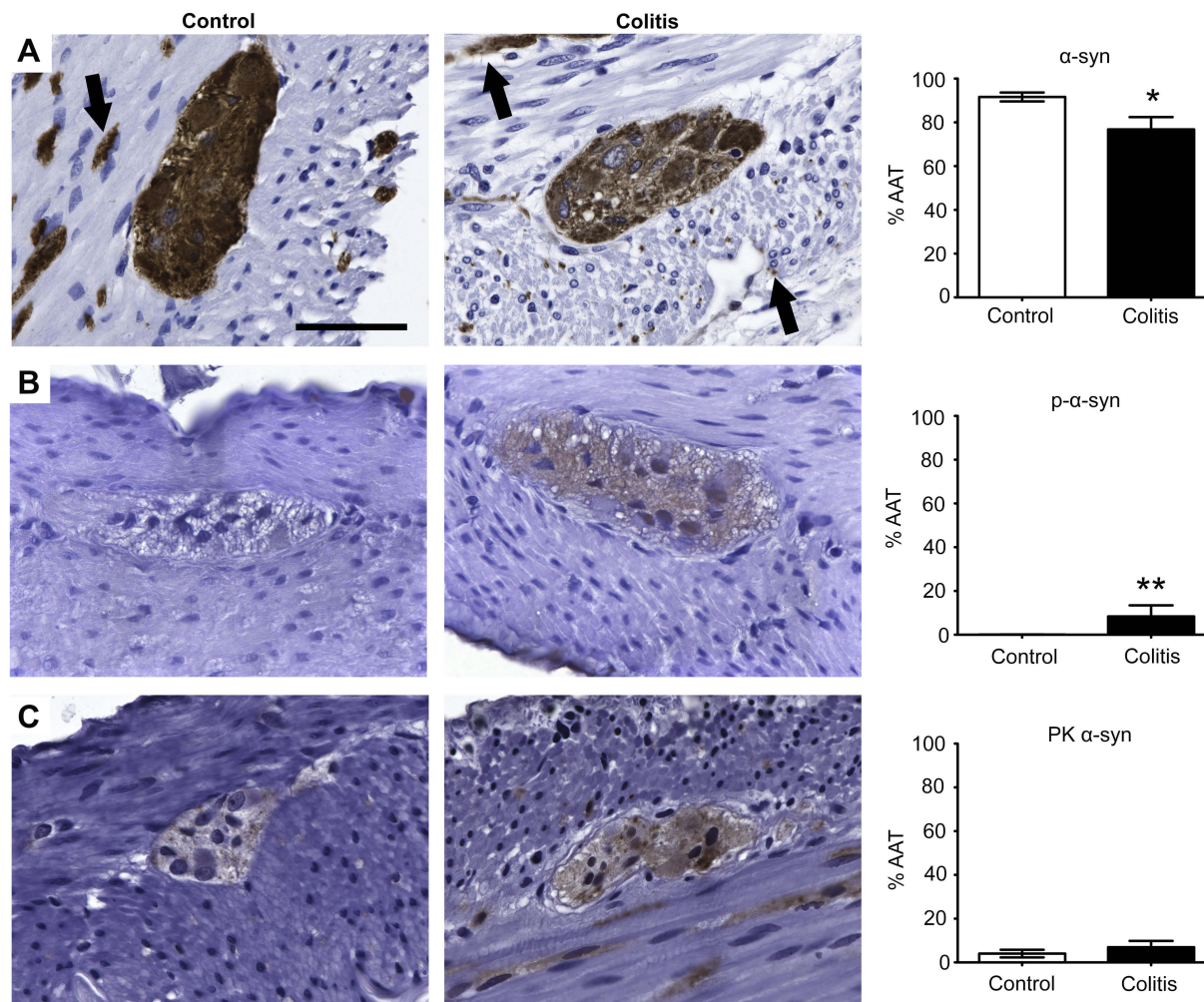
Figure 3 p-α-Syn expression was elevated in the colonic myenteric plexus of marmosets with colitis. Immunohistochemical staining of (**A**) α-syn, (**B**) p-α-syn, and (**C**) PK α-syn and quantification of percentage of total area of myenteric ganglia immunoreactive (%AAT) for each marker. Comparisons between groups were performed by either Student's *t*-test (α-syn and PK α-syn) or Mann–Whitney (p-α-syn) based on F-tests for equality of variances. α-Syn %AAT was significantly lower in colitis animals than controls (*p<0.04). p-α-Syn %AAT was significantly higher in colitis animals than controls (**p<0.02). PK α-syn was similar between groups (*p*>0.4). Scale bar =50 μm. n=5 per group. Black arrows (**A**) indicate nerve fibers.
Abbreviations: α-syn, alpha-synuclein; p-α-syn, α-syn phosphorylated at serine 129; PK α-syn, aggregated α-syn resistant to proteinase K treatment; %AAT, percent area above threshold.

Colitis did not affect general neuronal anatomy of myenteric ganglia as demonstrated by expression of PGP9.5. Studies in human patients suggest that ulcerative colitis (UC), one type of IBD, is associated with decreased myenteric neuron number as detected by HuC/D-ir.[24] In contrast, experimental murine colitis induced by drinking water supplemented with 3% dextran sulfate sodium for 7 days produced a significant increase in the number of enteric HuC/D-ir neurons.[25] The variable effects of colonic inflammation on the enteric neuronal population are likely related to the etiology and duration of colitis, such as the acute, chemical colitis induced by dextran sulfate sodium compared to the condition of UC. As in this marmoset study, multiple biopsies were not performed, the duration

of histologically defined colitis in the subjects is unknown. Despite the prevalence of GI dysfunction in PD[26] and the increase in pro-inflammatory cytokines in the colon of PD patients,[7] PD is not associated with changes in ENS neuronal number.[27,28]

The most common cause of GI disease in captive marmosets is chronic IBD of varying severity characterized by diffuse to segmental lymphocytic enteritis often termed chronic lymphocytic enteritis due to the presence of lymphocytic to lymphoplasmacytic inflammatory cells within the intestinal lamina propria.[29] Marmoset Wasting Syndrome (MWS),[30] includes the abovementioned GI conditions, yet in this report we refrained from using MWS as a diagnostic term, as MSW also includes tubulointerstitial
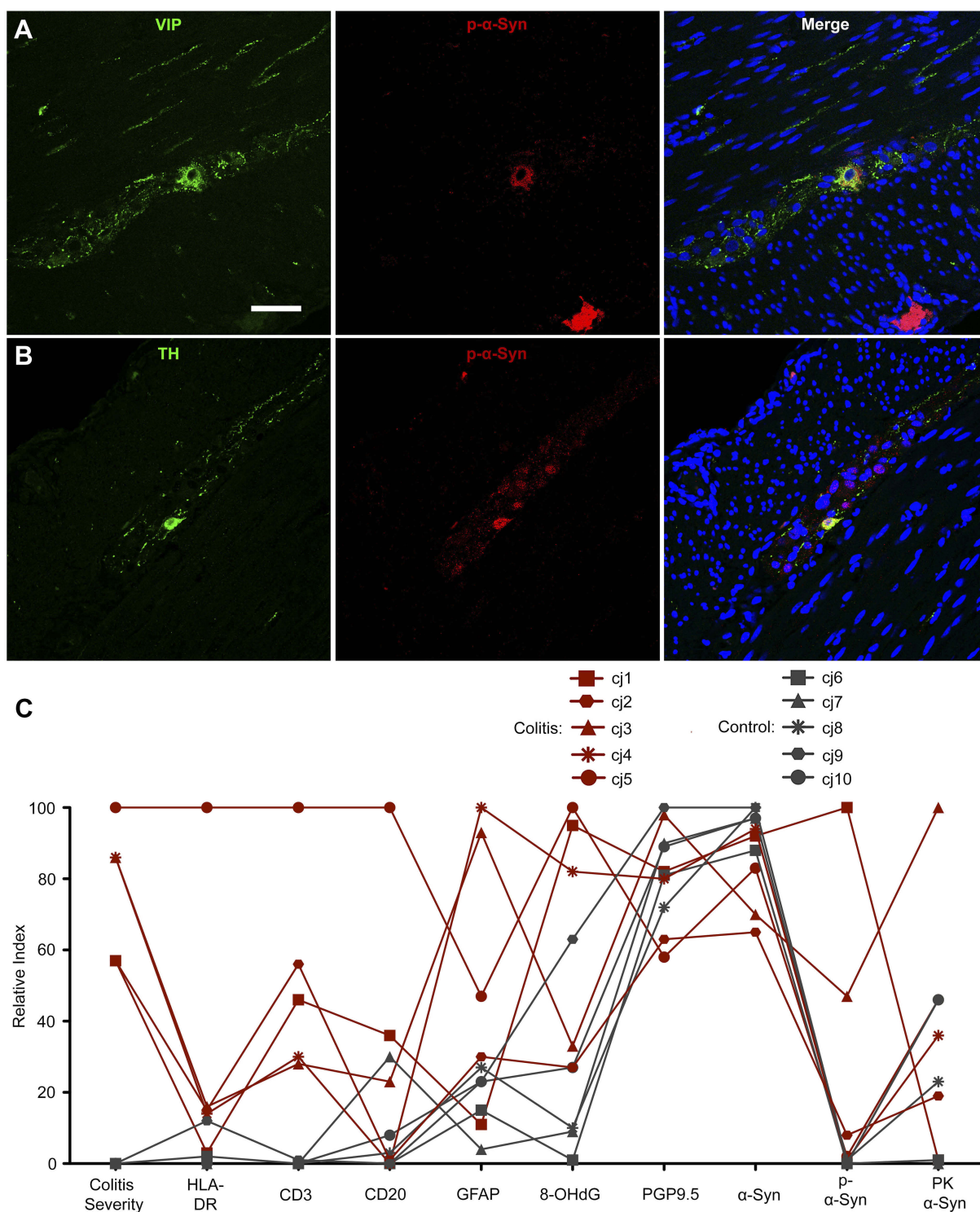
Figure 4 Phosphorylated α-syn was present in multiple myenteric neuronal populations in marmosets with colitis and comparing immunohistochemical markers in each animal reveals group and individual subject trends. (**A** and **B**) Immunofluorescent co-labeling of p-α-syn with (**A**) VIP or (**B**) TH in myenteric ganglia. Scale bar =50 μm. (**C**) Graph displaying colitis score and immunohistochemical marker data from each animal as percentage of maximum value (relative index) in each dataset.
Abbreviations: p-α-syn, alpha-synuclein phosphorylated at serine 129; VIP, vasoactive intestinal peptide; TH, tyrosine hydroxylase; HLA-DR, human leukocyte antigen DR; CD3, cluster of differentiation 3; CD20, cluster of differentiation 20; GFAP, glial fibrillary acidic protein; 8-OHdG, 8-hydroxy-2'-deoxyguanosine; PGP9.5, protein gene product 9.5; α-syn, alpha-synuclein; PK α-syn, aggregated α-syn resistant to proteinase K treatment.

nephritis, sarcopenia, hemosiderosis, and parasitism, with varying presentations in multiple species of marmosets and tamarins housed in captivity.[29] All subjects had gross

postmortem examinations with histology of all major organ systems (standard WNPRC practice) to assess for conditions associated with MWS and other pathologies

and were assigned final body condition and alopecia scores. Additional diagnostics, such as bacteriology, parasitology, or hematology were performed when possible. In this study, as in the majority of reported marmoset enteritis cases, colitis was largely idiopathic. Only one animal, cj5, tested positive at the time of postmortem examination for the O102 Shiga-toxin producing strain of *Escherichia coli*.[31] Cj2 had been diagnosed with giardia 3 years prior to death, resulting in prompt treatment and subsequent negative parasitology. Regardless of the cause, the reported marmoset colitis featured infiltration of antigen-presenting immune cells, including CD3+ T cells, into the myenteric ganglia, leading to increased gliosis and oxidative stress. This myenteric ganglionitis is also observed in human[32,33] and experimental[32,34] colitis. Similarly, gliosis is documented in human UC, infectious colitis,[35] and PD,[7,36] although reduced GFAP-ir is typical of Crohn's disease.[35]

A key finding of this study was the association between inflammation in the colon and alterations in myenteric α-syn, including increased α-syn S129 phosphorylation. Additionally, a decrease in myenteric ganglia α-syn %AAT was observed. Potential explanations for these findings include colitis-induced reduction of α-syn expression in myenteric ganglia or altered cellular distribution, potentially including oligomerization, of α-syn leading to decreased percent area of ganglia exhibiting α-syn-ir in colitis animals. It could be argued that the loss of α-syn expression in myenteric ganglia is due to neuronal loss. We were unable to perform unbiased stereological neuron cell counts, as this method requires tissue thickness greater than a neuronal nucleus and the thickness of the paraffin-embedded colonic sections was 5 um. Our lab has encountered this problem in the past,[23] and reported PGP9.5-ir as a representation of neuronal marker area in ganglia to validate the cell counts performed with HuC/D (a neuronal nuclear marker), as we did in this report. The results showed no difference in PGP9.5 across groups, suggesting that the colitis animals have "weaker" α-synuclein-ir with preservation of the myenteric neuronal population. As the PD field has historically focused on changes in catecholaminergic innervation, it should be noted that colonic myenteric ganglia TH+ neuronal cell bodies are rare and TH-immunoreactivity is located almost entirely in neuronal processes of extrinsic sympathetic innervation, thus the possibility that loss of TH+ neurons reducing α-synuclein-ir is very small. S129 phosphorylation is

associated with α-syn aggregation, although whether this post-translational modification promotes aggregate formation or resolution is still debated.[37] We did not detect a difference in levels of PK-resistant aggregated α-syn between groups in this study; it should be noted that it was difficult to achieve complete elimination of soluble α-syn using PK without extensive damage to the marmoset tissues. Due to rigorous tissue quality and subject health-based exclusion criteria, exact sex and age matching was difficult. Although no differences were noted between male and female subjects within either the control or colitis group, we recognize that the relatively small group size in this study precludes subgroup analysis or statistical analysis comparing males and females within a group.

A limitation of this study was the inability to assess for alterations in α-syn expression, phosphorylation, and aggregation in the central nervous system (CNS), as brain tissue from these animals was not available. Findings of LBs in the ENS of prodromal[38] or early stage PD patients have spurred the hypothesis that PD-associated α-syn pathology starts in the GI tract prior to retrograde travel from the ENS to the CNS via the vagus nerve.[39] Interestingly, recent work illustrates that enteroendocrine cells of the mucosal lining also express α-syn and provide an interface between the intestinal epithelium and ENS neurons, potentially serving as link between exposure to toxins or other environmental factors in GI contents and the initiation of α-syn pathology in the ENS.[40] Animal studies injecting different forms of α-syn (eg, monomeric, oligomeric, fibrillar) into the ENS have shown mixed results regarding caudo-rostral, trans-synaptic spreading of α-syn pathology to the CNS,[41–43] possibly due to the ability of recombinant α-syn monomers to form aggregates with varying biological activities.[41,44] However, evidence of truncal vagotomy decreasing the risk of developing PD[45,46] supports a role for the vagus nerve in PD pathogenesis. Additionally, the association between IBD and PD,[9–12] chronic *Helicobacter pylori* infection and PD,[47] the overlap in genetic risk factors between PD and Crohn's (*LRRK2, CARD15/NOD2* SNPs),[48] and a recent comprehensive epidemiological study describing decreased incidence of PD in patients that had appendectomies[49] illustrate a relationship between PD and GI tract health and function.

Overall, our report provides evidence for the hypothesis that colonic inflammation is capable of altering α-syn in the ENS. As we previously discussed, GI inflammation can be the consequence of several factors, including

infections. In that regard, increased α-syn expression was observed in the gut of aged rats orally administered *E. coli* producing the extracellular bacterial amyloid protein curli compared to non-curli-producing *E. coli*,[50] suggesting a role for individual bacterial proteins in α-syn pathology. Furthermore, pediatric patient small intestine biopsies showed increased α-syn-ir in submucosal enteric neurites with both acute and chronic inflammation and demonstrated an intra-patient increase in expression before and after norovirus infection.[51] α-Syn phosphorylation was not assessed in the aforementioned studies. Elucidating the mechanisms and timeline linking GI inflammation and PD pathology, including the role of specific pathogens or other factors in α-syn expression level, phosphorylation, and aggregation, will shed light on potential triggers of PD development.

Conclusion

The inflammation present in the proximal colon of common marmosets with naturally occurring colitis is sufficient to induce phosphorylation, but not aggregation, of α-syn in neurons of the myenteric plexus. Future work evaluating the vagus nerve and brains of animals with colitis will be key to revealing the contribution of colitis-induced ENS α-syn pathology to PD-like pathology in the brain.

Data Availability

The datasets generated during and/or analyzed during the current study are available from the corresponding author on reasonable request.

Acknowledgments

Disclosure

The authors report no conflicts of interest in this work.

References

1. Ford AC, Lacy BE, Talley NJ. Irritable bowel syndrome. *N Engl J Med*. 2017;376(26):2566–2578. doi:10.1056/NEJMra1607547
2. Abraham C, Cho JH. Inflammatory bowel disease. *N Engl J Med*. 2009;361(21):2066–2078. doi:10.1056/NEJMra0804647
3. Adelman DC, Murray J, Wu TT, Maki M, Green PH, Kelly CP. Measuring change in small intestinal histology in patients with celiac disease. *Am J Gastroenterol*. 2018;113(3):339–347. doi:10.1038/ajg.2017.480
4. Sheibani S, Gerson LB. Chemical colitis. *J Clin Gastroenterol*. 2008;42(2):115–121. doi:10.1097/MCG.0b013e318151470e
5. Papaconstantinou HT, Thomas JS. Bacterial colitis. *Clin Colon Rectal Surg*. 2007;20(1):18–27. doi:10.1055/s-2007-970196
6. Gecse KB, Vermeire S. Differential diagnosis of inflammatory bowel disease: imitations and complications. *lancet Gastroenterol hepatol*. 2018;3(9):644–653. doi:10.1016/S2468-1253(18)30159-6
7. Devos D, Lebouvier T, Lardeux B, et al. Colonic inflammation in Parkinson's disease. *Neurobiol Dis*. 2013;50:42–48. doi:10.1016/j.nbd.2012.09.007
8. Houser MC, Chang J, Factor SA, et al. Stool immune profiles evince gastrointestinal inflammation in Parkinson's Disease. *Mov Disord*. 2018;33(5):793–804. doi:10.1002/mds.27326
9. Weimers P, Halfvarson J, Sachs MC, et al. Inflammatory Bowel Disease and Parkinson's Disease: a nationwide swedish cohort study. *Inflamm Bowel Dis*. 2019;25(1):111–123. doi:10.1093/ibd/izy190
10. Villumsen M, Aznar S, Pakkenberg B, Jess T, Brudek T. Inflammatory bowel disease increases the risk of Parkinson's disease: a Danish nationwide cohort study 1977–2014. *Gut*. 2019;68(1):18–24. doi:10.1136/gutjnl-2017-315666
11. Zhu F, Li C, Gong J, Zhu W, Gu L, Li N. The risk of Parkinson's disease in inflammatory bowel disease: a systematic review and meta-analysis. *Dig Liver Dis*. 2018.
12. Peter I, Dubinsky M, Bressman S, et al. Anti-tumor necrosis factor therapy and incidence of parkinson disease among patients with inflammatory Bowel Disease. *JAMA Neurol*. 2018;75(8):939–946. doi:10.1001/jamaneurol.2018.0605
13. Lai SW, Liao KF, Lin CL, Sung FC. Irritable bowel syndrome correlates with increased risk of Parkinson's disease in Taiwan. *Eur J Epidemiol*. 2014;29(1):57–62. doi:10.1007/s10654-014-9878-3
14. Palma JA, Kaufmann H. Autonomic disorders predicting Parkinson's disease. *Parkinsonism Relat Disord*. 2014;20(Suppl 1):S94–S98. doi:10.1016/S1353-8020(13)70024-5
15. Gao X, Chen H, Schwarzschild MA, Ascherio A. A prospective study of bowel movement frequency and risk of Parkinson's disease. *Am J Epidemiol*. 2011;174(5):546–551. doi:10.1093/aje/kwr119
16. Vermilyea SC, Emborg ME. Alpha-synuclein and nonhuman primate models of Parkinson's disease. *J Neurosci Methods*. 2015;255:38–51. doi:10.1016/j.jneumeth.2015.07.025
17. Bendor JT, Logan TP, Edwards RH. The function of α-synuclein. *Neuron*. 2013;79(6):1044–1066. doi:10.1016/j.neuron.2013.09.004
18. Wakabayashi K, Tanji K, Odagiri S, Miki Y, Mori F, Takahashi H. The Lewy body in Parkinson's disease and related neurodegenerative disorders. *Mol Neurobiol*. 2013;47(2):495–508. doi:10.1007/s12035-012-8280-y
19. Unal-Cevik I, Gursoy-Ozdemir Y, Yemisci M, et al. Alpha-synuclein aggregation induced by brief ischemia negatively impacts neuronal survival in vivo: a study in [A30P]alpha-synuclein transgenic mouse. *J Cereb Blood Flow Metab*. 2011;31(3):913–923. doi:10.1038/jcbfm.2010.170
20. Acosta SA, Tajiri N, de la Pena I, et al. Alpha-synuclein as a pathological link between chronic traumatic brain injury and Parkinson's disease. *J Cell Physiol*. 2015;230(5):1024–1032. doi:10.1002/jcp.24830
21. Almandoz-Gil L, Welander H, Ihse E, et al. Low molar excess of 4-oxo-2-nonenal and 4-hydroxy-2-nonenal promote oligomerization of alpha-synuclein through different pathways. *Free Radic Biol Med*. 2017;110:421–431. doi:10.1016/j.freeradbiomed.2017.07.004

22. David JM, Dick EJ Jr., Hubbard GB. Spontaneous pathology of the common marmoset (Callithrix jacchus) and tamarins (Saguinus oedipus, Saguinus mystax). *J Med Primatol*. 2009;38(5):347–359. doi:10.1111/j.1600-0684.2009.00362.x

23. Shultz JM, Resnikoff H, Bondarenko V, et al. Neurotoxin-induced catecholaminergic loss in the colonic myenteric plexus of rhesus monkeys. *J Alzheimers Dis Parkinsonism*. 2016;6:6. doi:10.4172/2161-0460

24. Bernardini N, Segnani C, Ippolito C, et al. Immunohistochemical analysis of myenteric ganglia and interstitial cells of Cajal in ulcerative colitis. *J Cell Mol Med*. 2012;16(2):318–327. doi:10.1111/j.1582-4934.2011.01298.x

25. Belkind-Gerson J, Hotta R, Nagy N, et al. Colitis induces enteric neurogenesis through a 5-HT4-dependent mechanism. *Inflamm Bowel Dis*. 2015;21(4):870–878. doi:10.1097/MIB.0000000000000326

26. Cheon SM, Ha MS, Park MJ, Kim JW. Nonmotor symptoms of Parkinson's disease: prevalence and awareness of patients and families. *Parkinsonism Relat Disord*. 2008;14(4):286–290. doi:10.1016/j.parkreldis.2007.09.002

27. Annerino DM, Arshad S, Taylor GM, Adler CH, Beach TG, Greene JG. Parkinson's disease is not associated with gastrointestinal myenteric ganglion neuron loss. *Acta Neuropathol*. 2012;124(5):665–680. doi:10.1007/s00401-012-1040-2

28. Corbille AG, Coron E, Neunlist M, Derkinderen P, Lebouvier T. Appraisal of the dopaminergic and noradrenergic innervation of the submucosal plexus in PD. *J Parkinsons Dis*. 2014;4(4):571–576. doi:10.3233/JPD-140422

29. Ludlage E, Mansfield K. Clinical care and diseases of the common marmoset (Callithrix jacchus). *Comp Med*. 2003;53(4):369–382.

30. Otovic P, Smith S, Hutchinson E. The use of glucocorticoids in marmoset wasting syndrome. *J Med Primatol*. 2015;44(2):53–59. doi:10.1111/jmp.12159

31. Perepelov AV, Wang Q, Senchenkova SN, et al. Structure and gene cluster of the O-antigen of Escherichia coli O102. *Carbohydr Res*. 2012;361:73–77. doi:10.1016/j.carres.2012.07.024

32. Lakhan SE, Kirchgessner A. Neuroinflammation in inflammatory bowel disease. *J Neuroinflammation*. 2010;7:37. doi:10.1186/1742-2094-7-59

33. Tornblom H, Lindberg G, Nyberg B, Veress B. Full-thickness biopsy of the jejunum reveals inflammation and enteric neuropathy in irritable bowel syndrome. *Gastroenterology*. 2002;123(6):1972–1979. doi:10.1053/gast.2002.37059

34. Pontell L, Castelucci P, Bagyanszki M, et al. Structural changes in the epithelium of the small intestine and immune cell infiltration of enteric ganglia following acute mucosal damage and local inflammation. *Virchows Arch*. 2009;455(1):55–65. doi:10.1007/s00428-009-0795-x

35. von Boyen GB, Schulte N, Pfluger C, Spaniol U, Hartmann C, Steinkamp M. Distribution of enteric glia and GDNF during gut inflammation. *BMC Gastroenterol*. 2011;11:3. doi:10.1186/1471-230X-11-93

36. Clairembault T, Kamphuis W, Leclair-Visonneau L, et al. Enteric GFAP expression and phosphorylation in Parkinson's disease. *J Neurochem*. 2014;130(6):805–815. doi:10.1111/jnc.12742

37. Oueslati A. Implication of alpha-synuclein phosphorylation at S129 in synucleinopathies: what have we learned in the last decade? *J Parkinsons Dis*. 2016;6(1):39–51. doi:10.3233/JPD-160779

38. Hilton D, Stephens M, Kirk L, et al. Accumulation of alpha-synuclein in the bowel of patients in the pre-clinical phase of Parkinson's disease. *Acta Neuropathol*. 2014;127(2):235–241. doi:10.1007/s00401-013-1214-6

39. Braak H, de Vos RA, Bohl J, Del Tredici K. Gastric alpha-synuclein immunoreactive inclusions in Meissner's and Auerbach's plexuses in cases staged for Parkinson's disease-related brain pathology. *Neurosci Lett*. 2006;396(1):67–72. doi:10.1016/j.neulet.2005.11.012

40. Chandra R, Hiniker A, Kuo YM, Nussbaum RL, Liddle RA. alpha-Synuclein in gut endocrine cells and its implications for Parkinson's disease. *JCI Insight*. 2017;2:12. doi:10.1172/jci.insight.88864

41. Uemura N, Yagi H, Uemura MT, Hatanaka Y, Yamakado H, Takahashi R. Inoculation of alpha-synuclein preformed fibrils into the mouse gastrointestinal tract induces Lewy body-like aggregates in the brainstem via the vagus nerve. *Mol Neurodegener*. 2018;13(1):21. doi:10.1186/s13024-018-0257-5

42. Manfredsson FP, Luk KC, Benskey MJ, et al. Induction of alpha-synuclein pathology in the enteric nervous system of the rat and non-human primate results in gastrointestinal dysmotility and transient CNS pathology. *Neurobiol Dis*. 2018;112:106–118. doi:10.1016/j.nbd.2018.01.008

43. Pan-Montojo F, Schwarz M, Winkler C, et al. Environmental toxins trigger PD-like progression via increased alpha-synuclein release from enteric neurons in mice. *Sci Rep*. 2012;2:898. doi:10.1038/srep00386

44. Peng C, Gathagan RJ, Lee VM. Distinct alpha-Synuclein strains and implications for heterogeneity among alpha-Synucleinopathies. *Neurobiol Dis*. 2018;109(Pt B):209–218. doi:10.1016/j.nbd.2017.07.018

45. Svensson E, Horvath-Puho E, Thomsen RW, et al. Vagotomy and subsequent risk of Parkinson's disease. *Ann Neurol*. 2015;78(4):522–529. doi:10.1002/ana.24448

46. Liu B, Fang F, Pedersen NL, et al. Vagotomy and Parkinson disease: a Swedish register-based matched-cohort study. *Neurology*. 2017;88(21):1996–2002. doi:10.1212/WNL.0000000000003961

47. Nielsen HH, Qiu J, Friis S, Wermuth L, Ritz B. Treatment for Helicobacter pylori infection and risk of Parkinson's disease in Denmark. *Eur J Neurol*. 2012;19(6):864–869. doi:10.1111/j.1468-1331.2011.03643.x

48. Houser MC, Tansey MG. The gut-brain axis: is intestinal inflammation a silent driver of Parkinson's disease pathogenesis? *NPJ Parkinsons Dis*. 2017;3:3. doi:10.1038/s41531-016-0002-0

49. Killinger BA, Madaj Z, Sikora JW, et al. The vermiform appendix impacts the risk of developing Parkinson's disease. *Sci Transl Med*. 2018;10:465. doi:10.1126/scitranslmed.aao4496

50. Chen SG, Stribinskis V, Rane MJ, et al. Exposure to the functional bacterial amyloid protein curli enhances alpha-synuclein aggregation in aged fischer 344 rats and caenorhabditis elegans. *Sci Rep*. 2016;6:34477. doi:10.1038/srep34477

51. Stolzenberg E, Berry D, Yang D, et al. A role for neuronal alpha-synuclein in gastrointestinal immunity. *J Innate Immun*. 2017;9(5):456–463. doi:10.1159/000477990

Supplementary materials
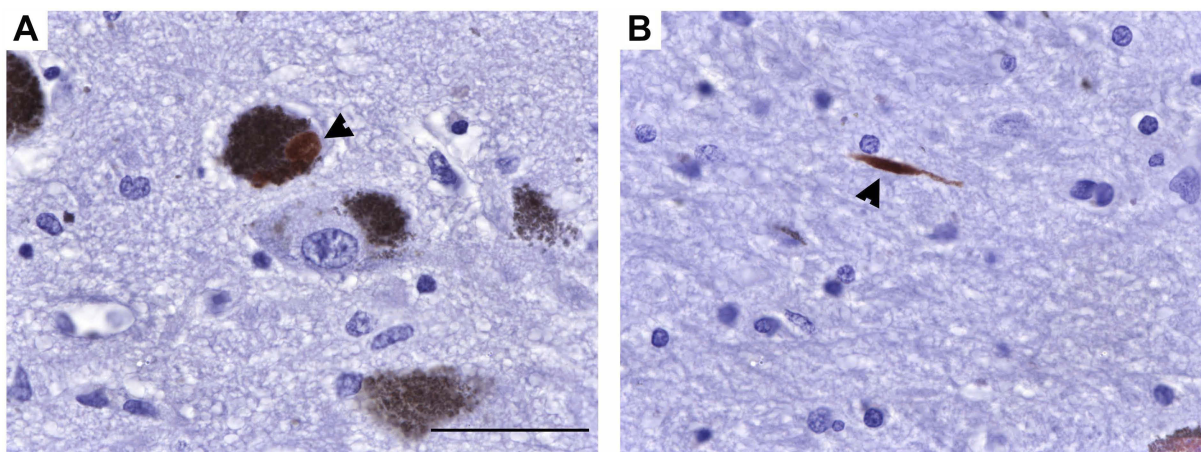
Figure S1 S129 phosphorylated α-syn in a sample of brain from a human PD patient. (**A** and **B**) Representative photomicrographs at 63× of p-α-syn-ir in human PD brain in (**A**) a neuromelanin laden neuron and (**B**) a neurite. Scale bar =50 μm.
Abbreviations: p-α-syn-ir, S129 phosphorylated alpha-synuclein- immunoreactivity; PD, Parkinson's disease.
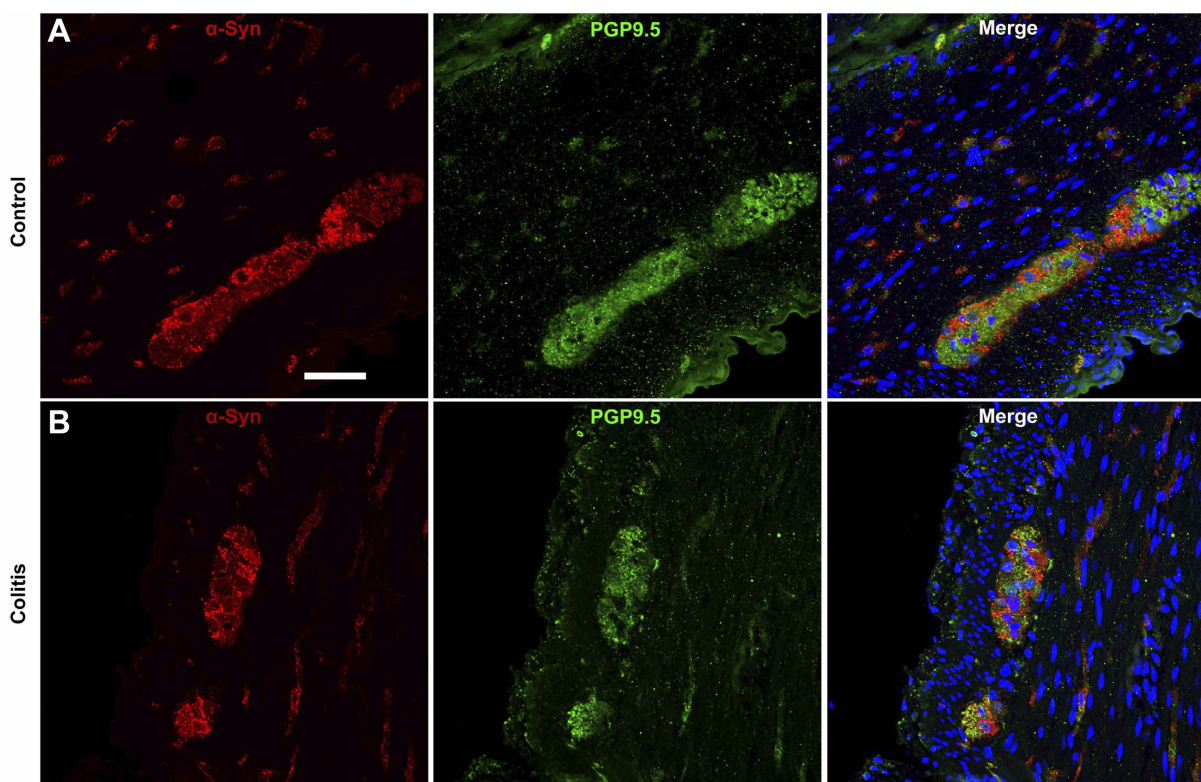
Figure S2 α-Syn co-labeling with the panneuronal marker PGP9.5 in myenteric ganglia is similar in control and colitis animals. (**A** and **B**) Representative photomicrographs at 40× showing immunofluorescent co-labeling of α-syn and PGP9.5 in myenteric ganglia and nerve fibers in (**A**) control and (**B**) colitis animals. Note that small punctate spots in the PGP9.5 immunofluorescence are technical artifact/background. Scale bar =50 μm.
Abbreviations: α-syn, alpha-synuclein; PGP9.5, protein gene product 9.5.